Selection of the Flat Field Calibration System Beam Speed

Date:	October 18, 2000
Document Number:	COS-11-0015
Revision:	Revision A
Contract No.:	NAS5-98043
CDRL No.:	N/A

Prepared By:	Erik Wilkinson	
	E. Wilkinson, COS Instrument Scientist, CU/C	
Reviewed By:	Kim MacFeeley	4/6/00
	R. Cahill, Optical Des	Date
Reviewed By:	James C. Green	4/6/00
	J. Green, COS Principal Investigator, CU/CAS	Date
Reviewed By:	Dennis Ebbets	4/6/00
	D. Ebbets, Calibration Scient	Date
Approved By:	J. Andrews	4/6/00
	J. Andrews, COS Experiment Manager, CU/CASA	Date
Approved By:	Don Hood	4/6/00
	D. Hood, Program Manager, BATC	Date

Center for Astrophysics & Space Astronomy
University of Colorado
Campus Box 593
Boulder, Colorado 80309

REVISIONS

Letter	ECO No.	Description	Check	Approved	Date
-		Initial Release		EW	3/23/00
A	COS-043	Changes detailed on redlined copy attached to ECO			

Original Release Name	Date
Drawn: E. Wilkinson	3/17/00
Reviewed:	
Approved:	

THE UNIVERSITY OF COLORADO
At Boulder
The Center for Astrophysics and Space Astronomy

Selection of the Flat Field
Calibration System Beam Speed

Size	Code Indent No.	Document No.	Rev
A		COS-11-0015	A
Scale: N/A			

Table of Contents

1. INTRODUCTION

This document reports the results of an investigation of the effects of the beam speed of the flat field calibration system on system performance. Based on the results of this study we recommend that the beam speed for the flat field calibration system is F/24, however, allowing for an aperture stop to slow down the beam may be advantageous.

2. RAYTRACE MODELING & ANALYSIS

The investigation was conducted using full IRT raytrace models of the COS FUV G130M and NUV G185M channels. In the raytrace models a cone of light with a variable beam speed uniformly illuminates the flat field aperture. For each case 100 wavelengths separated by 1Å and centered on 1300Å and 1850Å respectively were raytraced. For each wavelength 1000 rays were passed through the system for a total of approximately 10^5 photons.

Figure 1 is the spot diagram for the G130M grating assuming an F/12 input beam to the flat field aperture. Figures 2 and 3 show the histograms of image in the dispersion and cross-dispersion directions. Figure 1 and 2a show that the flat field system is producing a uniformly illuminated stripe across the spectral region. In the cross-dispersion direction the distribution distributes light across the entire detector with about 40% of the counts falling in the spectral region.

Figures 1, 2, and 3 highlight the impetus for this trade study. With an F/12 input beam roughly 60% of the photons lie outside the spectral region. These photons will contribute the majority of deadtime to the flat field observation with no benefit. Furthermore, the photons outside the spectral region will extract charge from regions outside the spectral area. It has always been the philosophy of the COS IDT to expose only the spectral region of the detector to photons so as to minimize the charge extraction from both a local and global perspective. As charge is extracted from the MCPs during routine observations the spectrum will be moved to pristine areas as required to maintain the detection quantum efficiency of the COS FUV detector. Therefore, understanding how the F# would lead to unwanted exposure of these pristine areas is important.

Four raytrace models were run for each channel. Only the input beam speed was varied between each model. The input beam speeds used were F/12, F/16, F/24, & F/48. Figures 4 and 5 show the histograms in the cross-dispersion direction for the FUV and NUV channels respectively as functions of beam speed.

The first metric for analyzing the results in figure 4 is to compare the counts within the spectral region to those counts outside the spectral region. The spectral region was defined as the ±0.5mm centered on the peak of the distribution. The results are shown in Table 1. The low percentage of counts within the spectral region for the F/24 case is unacceptable because at a constant flux level it will take more than twice as long to accumulate a flat field than it will for the F/24 case.

Table 1

	Counts		
F#	**In spectral regions**	**Total**	**% in spectral region**
12	41412	97061	43
16	65229	97061	67
24	91947	97061	95
48	97056	97061	100

The next issue to examine is how much charge is extracted from the regions outside the spectral area. To do this I calculated the counts/mm inside and outside of the spectral region and formed the ratio of these two values. This ratio can be thought of as a contrast metric. A large ratio means that the density of counts outside the spectrum is lower than inside the spectrum. The results are in Table 2. The counts/mm inside (CI) and outside (CO) the spectrum were calculated using equations 1 and 2 respectively. The 60 represents the illuminated portion of the detector in the spectral direction in the raytrace simulations (60 mm, see Figure 1).

$$CI = \frac{a}{60 \cdot 1} \tag{1}$$

$$CO = \frac{b}{60 \cdot (\frac{A}{2} - 0.5)} \tag{2}$$

Based on the preliminary lifetime results of the COS microchannel plate samples the current plan is to limit the number of high quality flat fields to two per year. If the ratio CI/CO~4 then two flat fields will extract as much charge as half a flat field. Based on the CASA-11-0012 the ratio of the total number of photons in two flat fields to the total number of astrophysical photons in 1 year is 4.9. This indicates that for the F/12 and F/16 cases the photons outside the spectral region would have the same effect on the microchannel plate lifetime as observing for 1 year. Choosing a ratio of CI/CO ≥10 insure that flat field data will not compromise the microchannel plate lifetime outside the spectral region with a factor of 2 margin.

Table 2

	Counts			*area outside (A)*	**Counts/mm**		*ratio*
F#	*Inside(a)*	*outside(b)*	*total*		*Inside(CI)*	*Outside(CO)*	
12	41412	16100	97061	10.9	690	187	3.7
16	65229	9000	97061	5.1	1087	258	4.2
24	91947	1200	97061	2.1	1532	155	10
48	97056	0	97061	1	1617	0	∞

Note how the ratios for the F/12 and F/16 cases are essentially identical. This indicates that there would be the same count density outside the spectral region for both cases, although the total number of photons inside the spectral region would be much higher. At F/24 the ratio jumps to 10, thus indicating that the photon density outside the spectral region is substantially lower and so less charge would be extracted in the pristine areas.

The flat field calibration system by design is an imperfect system, as it does not simulate the aberrations of the HST OTA. To evaluate this issue I compared the histogram in y for a full F/12 beam with this histogram of an F/12 with the central F/24 missing (see Figure 6). We immediately see that the tight component in Figures 3, 5, and 6 comes from the light within the F/24 cone. The light outside the F/24 cone fills the entire detector with only an enhancement towards the center of the detector, but not the tight core. Figure 6 demonstrates that the flat field system should be F/24 or slower, as the light for beam speeds faster than F/24 only illuminate regions outside the region of interest.

3. CONCLUSIONS

Based on the results presented above the F/24 beam speed is the best choice for the flat field calibration subsystem. The majority of the photons injected into the system will land in the spectral region, so the observing efficiency in this mode will be maximized. The few counts that do fall outside the spectral region will not compromise the lifetime of the microchannel plates for future use.

There are a few open issues that must be considered and resolved as the COS instrument is assembled. First, by limiting the F# of the flat field to F/24 the flux will also be limited. This may length the integration times for a flat field exposure. As the radiometry data becomes available for the D2 flat field lamp this issue will be resolved.

Another issue regarding the flat field has been raised by FUSE project that is relevant for COS. The illumination of the flat field should be as similar to the standard light path as possible. This is especially crucial for the grid shadowing which is dependent upon the illuminating F# and the angular extent of the object in the field of view. There is no clear resolution of these issues at this time, but they must be considered and accounted for during instrument integration, test, and calibration.

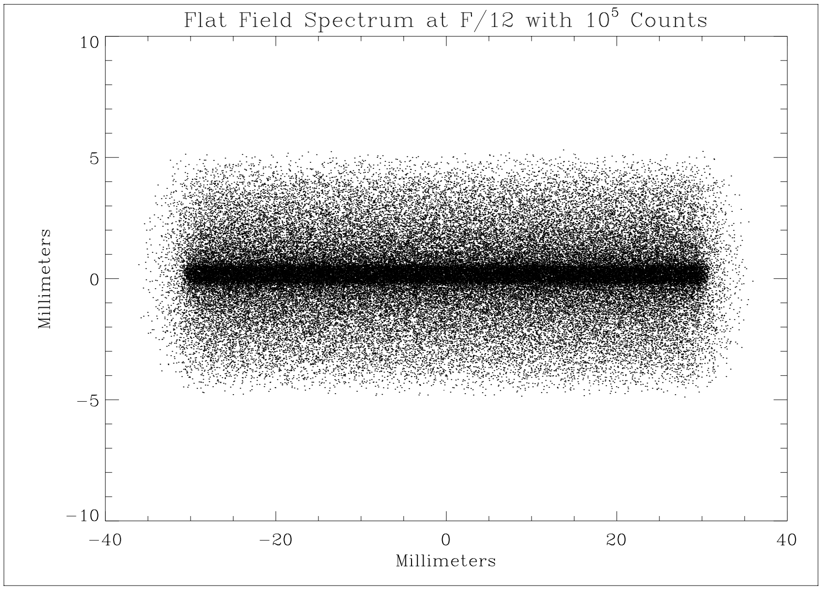

Figure 1: Spot diagram of 100Å centered at 1300 Å in the G130M channel.

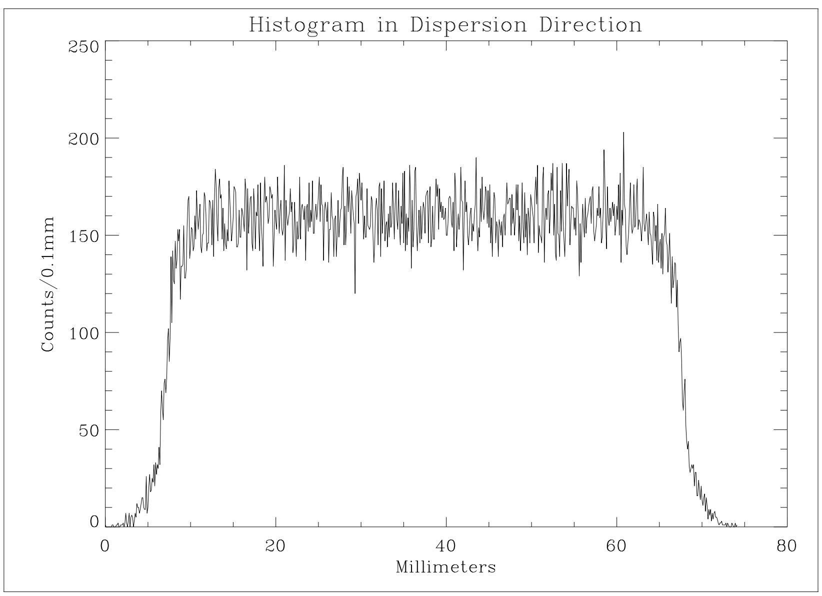

Figure 2: Histogram of the spot diagram in the dispersion direction.

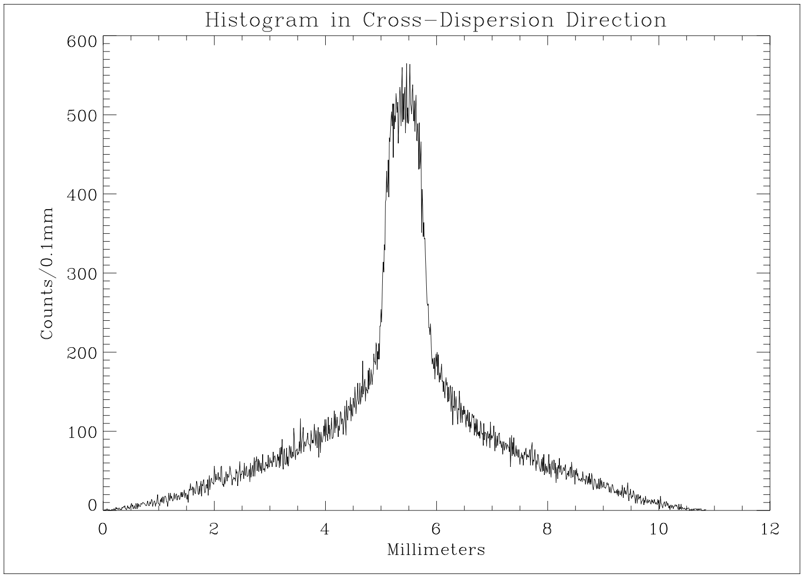

Figure 3: Histogram in the cross-dispersion direction.

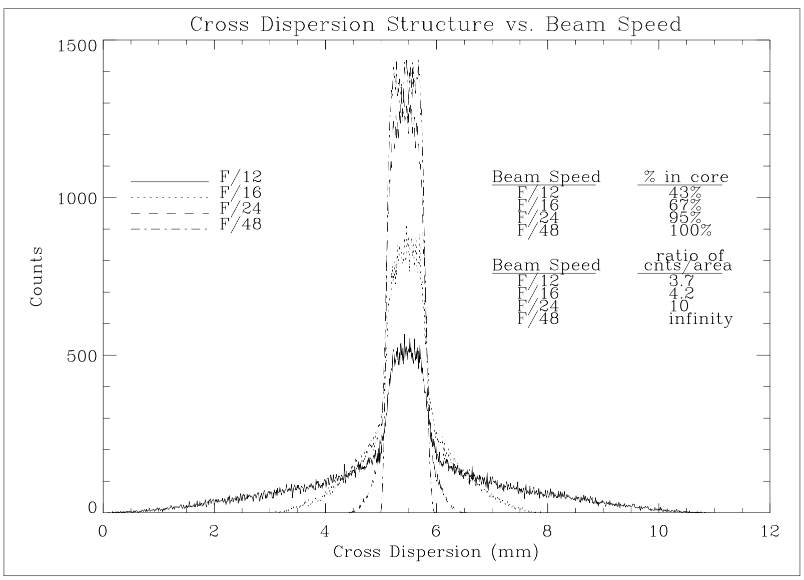

Figure 4: Comparison of histograms in the cross-dispersion direction of the flat field calibraiton system through the G130M channel for various F#s.

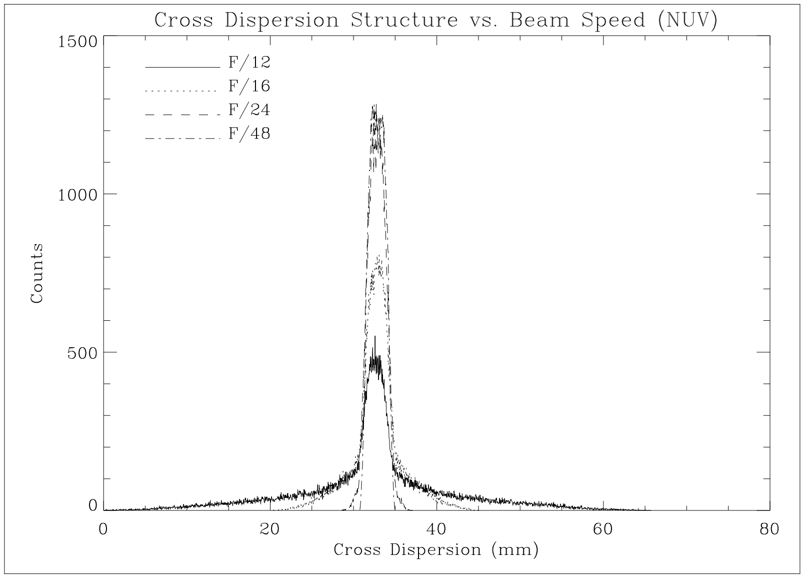

Figure 5: Comparison of histograms in the cross-dispersion direction of the flat field calibraiton system through the G185 channel for various F#s.

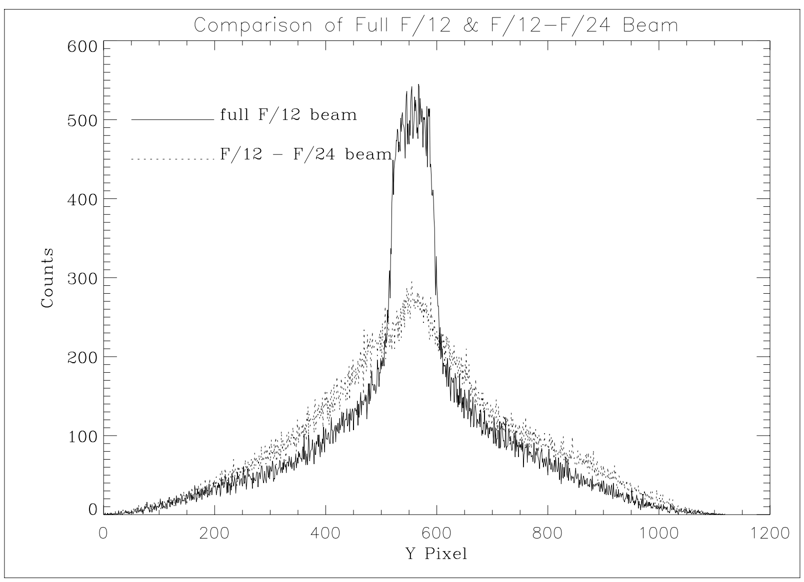

Figure 6: Comparison of histograms for a full F/12 beam and an F/12 beam missing the central F/24 portion of the beam.